Journal of *Marine Science and Engineering*

MDPI

Article

Towards Lower Carbon Emissions: A Distributed Energy Management Strategy-Based Multi-Objective Optimization for the Seaport Integrated Energy System

Yuxin Zhang [1], Yang Xiao [2,*], Qihe Shan [1] and Tieshan Li [3]

[1] Navigation College, Dalian Maritime University, Dalian 116026, China; zyx97_dlmu@163.com (Y.Z.); shanqihe@dlmu.edu.cn (Q.S.)
[2] Department of Computer Science, The University of Alabama, Tuscaloosa, AL35487-0290, USA
[3] School of Automation Engineering, University of Electronic Science and Technology of China, Chengdu 611731, China; tieshanli@126.com
* Correspondence: yangxiao@ieee.org

Abstract: To decrease fuel-based energy consumption, it is important to investigate the optimal energy management problem for the seaport integrated energy system in a fully distributed manner. A multi-objective energy management model is constructed, considering energy consumption, greenhouse gas emission, and carbon trading, which satisfy the sustainable development of the international shipping industry advocated by the International Maritime Organization (IMO). The carbon exhaust of a seaport is restrained by integrated carbon capture/storage devices. A fully distributed energy management strategy with dynamic-weighted coefficients is proposed to acquire the optimal solutions for the seaport integrated energy system. Moreover, to decrease the communication resources, an event-triggered mechanism between energy bodies was designed against the bandwidth limitation of the seaport. Finally, a rigorous mathematical analysis based on the multi-agent theory and the case studies proves the effectiveness of the proposed method.

Keywords: seaport integrated energy system; distributed multi-objective optimization; energy management; greenhouse gas emission

Citation: Zhang, Y.; Xiao, Y.; Shan, Q.; Li, T. Towards Lower Carbon Emissions: A Distributed Energy Management Strategy-Based Multi-Objective Optimization for the Seaport Integrated Energy System. *J. Mar. Sci. Eng.* **2023**, *11*, 681. https://doi.org/10.3390/jmse11030681

Academic Editor: Theocharis D. Tsoutsos

Received: 8 March 2023
Revised: 18 March 2023
Accepted: 21 March 2023
Published: 22 March 2023

1. Introduction

As one of the most significant parts of international trade, seaports operate at a great capacity and consume a large number of primary energy sources. In the past decade, the amount of greenhouse gases emitted by seaports has accounted for 3–5% of the total global emissions. To improve energy efficiency and reduce carbon emissions, research has been conducted on seaports [1,2].

To limit the carbon footprint, various measures have been implemented to reduce negative environmental impact, and these measures are gradually being applied to practical seaport engineering projects [3]. The European Union Emissions Trading System (EU-ETS) was introduced in 2003 as the world's first multinational emissions-trading scheme. It promotes carbon trading among more than 30 member countries and treats carbon emission permits as a circulating commodity [4]. The navigation industry, greatly supporting international trade, was included in the carbon emission trading system in 2022. Meanwhile, the goal of "Fit for 55" was supplemented, regulating the indirect costs of carbon trading involving ships and seaports. To this end, the monitoring–reporting–verification (MRV) mechanism for carbon dioxide emissions was established by the European Union (EU) [5]. It promotes the carbon trading market effectively. Moreover, many major seaports worldwide, such as Hamburg, Kiel, and Barcelona, propose using seaports as independent energy unions to realize reasonable energy management. Considering that the power, heating, and gas networks are closely coupled into the seaport, the seaport can be commonly

viewed as an integrated energy system [6,7]. In order to study how to allocate multi-energy supplements and meet the diversified energy load cooperatively, the energy management problem (EMP) of the seaport integrated system should be a concern [8,9].

The EMP has been focused on in recent years as part of fundamental research. Many algorithms have been studied to solve the EMP, which can be divided into centralized and distributed methods [10,11]. With the development of renewable technologies, more non-professional energy producers have been applied to the seaport integrated energy system. This suggests that traditional centralized methods are not adaptable to the increasingly complex seaport integrated energy system. To decrease the total operation costs, a multi-agent cooperative control mechanism was designed for the renewable energy-powered multi-energy hub system [12]. To achieve energy management and ensure the reliability of the integrated energy system, simultaneously, [13] investigated the distributed-based economic dispatch strategy. Moreover, to acquire the optimal trading solution, a distributed resilient double-gradient descent-based energy management algorithm was proposed [14]. The above research studies considered minimal operation costs as the optimal objective while satisfying various local operation constraints.

However, according to the procedures released by the International Maritime Organization (IMO), noxious gas emissions must be limited in control areas [15,16]. IMO's policy framework of environmental protection can be divided into three categories, namely, planning and guidance policies, mandatory and restrictive policies, and support and guarantee policies [17]. The greenhouse gas reduction of navigation was first advocated in the 23rd assembly of the IMO in 2003. Meanwhile, to implement the blueprint of energy conservation and decrease the navigation's carbon intensity, a draft of the initial IMO Strategy on the Reduction of GHG Emissions from Ships was adopted in 2018 [18,19]. Moreover, many amendments were approved by the Marine Environment Protection Committee (MEPC) in 2020 and 2021. To this end, conventional energy management models, depending on operational costs only, will be unsuitable for the upcoming seaport integrated energy system [20,21]. Therefore, a multi-objective energy management model, considering the environmental protection and economic benefits, should be investigated to support Sustainable Development Goal 13, advocated by the United Nations (UN). To ensure energy-efficient trading of residential grid-connected PV-battery hybrid systems, a multi-objective energy management strategy was proposed based on a three-level control mechanism [22]. Meanwhile, an improved energy management model was constructed to reduce the operational costs and the storage utilization of the hybrid microgrid [23]. Previous research studies have successfully achieved energy management with a low carbon footprint; the obtained optimal energy management solutions can be employed in theory and practice. This may suggest that those works depended on updated communication among energy participants.

Specifically, existing ship–seaport communication systems have different bandwidths, incompatible formats, and inconsistent signal transmission stability [24]. Moreover, considering the complex marine environment, especially within 15–30 km offshore, the communication quality between the ship and the seaport is vulnerable [25]. Therefore, the communication bandwidth is limited for the seaport integrated energy system [26]. On this basis, to deal with the communication limitations of the seaport, an event-triggered communication mechanism is necessary [27]. It can avoid the waste of vigorous computations and communications resulting from the continuous communication between energy participants [28], which is suitable for the flexible and autonomous seaport integrated energy system. Moreover, the communication resources can be effectively saved without successive and real-time communication mechanisms. As for multi-energy systems with energy bodies, an event-triggered-based distributed strategy has been designed to achieve maximal social welfare [29]. Additionally, although the idea of an event-triggered communication mechanism has been introduced into the EMP, the employed mechanism cannot meet the complex–regional multi-objective energy management of the seaport integrated energy system.

With the motivations analyzed above, to decrease the negative impacts of carbon emission caused by the normal operation of the seaport, it is necessary to take the greenhouse

gas emission, and carbon trading into consideration [30,31]. The multi-objective energy management pattern of the seaport integrated energy system involves the comprehensive allocation of resources under the needs of the economy and environment, which is disparate from the single-objective optimization of economic benefits [32,33]. Furthermore, in order to increase the efficiency of communication resources, event-triggered mechanisms between energy entities are effective at overcoming bandwidth limitations that frequently occur in seaport integrated systems [34,35]. Therefore, the multi-objective energy management problem, which includes economic and environmental benefits under a discrete communication mechanism, is important to meet the sustainable development of the international shipping industry; this is important to comply with the 'Future Fuels and Technology for Low and Zero-Carbon Shipping Project (FFT Project)' advocated by the IMO.

(1) To adapt sustainable marine developments, as advocated by the IMO, a multi-objective energy management model for the seaport integrated energy system was established. Furthermore, the dynamic-weighted coefficient was designed to reconstruct the multi-objective EMP as a single objective scheduling problem, reducing the EMP complexity. Moreover, the constructed seaport energy management model performs well in the overall consideration of energy consumption costs, greenhouse gas emissions, and carbon trading, effectively decreasing pollution emissions.

(2) A fully distributed seaport energy management strategy proposed by the multi-agent average consensus theory was designed to deal with the EMP of the seaport integrated energy system. Moreover, an event-triggered communication mechanism was constructed into the distribution strategy in response to the seaport's bandwidth limitation. The seaport's optimal energy management solution can be obtained with lower communication resources, which greatly decreases the operation costs of the seaport. Moreover, the positive minimal inter-event was proved by introducing an auxiliary term; the discrete nonlinear system theory verifies the convergence of the incremental cost.

The remainder of this paper is organized as follows. Section 2 introduces the structure and devices of the seaport integrated energy system. The multi-objective energy management model and the fully distributed strategy with the event-triggered mechanism are presented in Section 3. In Section 4, numerical case studies are presented to verify the effectiveness of the theorems. Section 5 concludes the paper. Moreover, a discussion of the theorems is presented in Appendix A.

2. Energy Management for Seaport Integrated Energy System

In this section, the structure of the seaport integrated energy system is analyzed. As shown in Figure 1, the considered seaport integrated energy system comprises the power, heating, and gas networks. The node sequence set of the seaport integrated energy system is denoted as $C = C_P \cup C_H \cup C_G$, where C_P, C_H, C_G are the node sequence sets of power, heating, and gas, respectively.

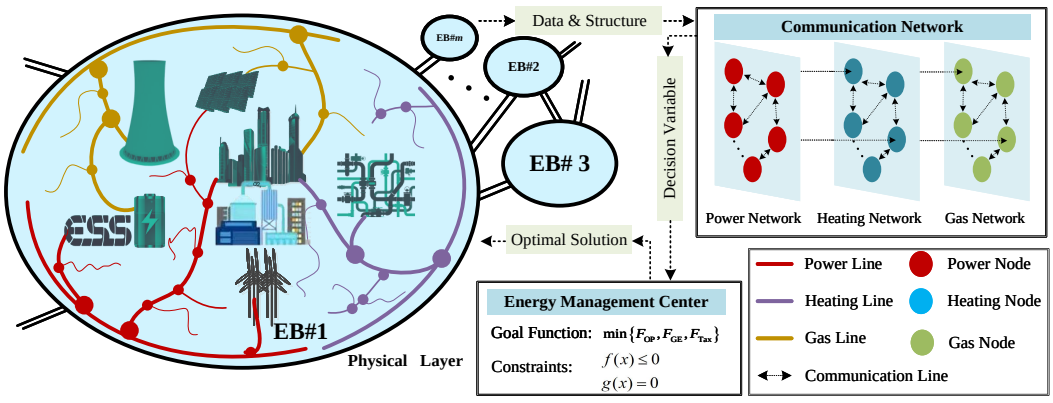

Figure 1. Basic structure of the seaport integrated energy system.

2.1. Structure of the Seaport Integrated Energy System

Normally, the seaport can be classified into various areas based on the types of cargo, loads–unload facilities, and energy participants. The regional operation distribution of the seaport is essential for improving operational efficiency. The integration of energy generation and consumption devices within the energy body (EB) forms the fundamental structure of the seaport's integrated energy system. We assume that there are m energy bodies in the seaport integrated energy system, which contains n_z^p power nodes, n_z^h heating nodes, and n_z^g gas nodes in the zth EB, respectively, for $\forall z \in \Omega_{\mathrm{m}} = \{1, 2, ..., m\}$. Specifically, $\sum_{z=1}^{m} n_z^p = \mathrm{N_P}$, $\sum_{z=1}^{m} n_z^h = \mathrm{N_H}$, and $\sum_{z=1}^{m} n_z^g = \mathrm{N_G}$, where N_{P}, N_{H}, and N_{G} are the node numbers of the power, heating, and gas networks, respectively. Furthermore, the positive direction of the energy injection at each node is defined as the direction from the generator and load to the node.

Carbon capture and carbon storage technologies are considered with the seaport integrated energy system reform. Since the innovative technologies and renewable devices, greenhouse gas emissions exhausted by the traditional diesel generators of the seaport energy system can be effectively reduced. Specifically, carbon emissions can be captured with less exhaust into the atmosphere. Moreover, the stored carbon can be converted into raw material to support the gas network and generate other resources. Meanwhile, the seaport integrated energy system (with its energy bodies) has great autonomy and regionality; therefore, the conventional communication network cannot deal with the mass amounts of data gathered from diversified energy networks. To overcome the drawbacks, the seaport integrated energy system was designed, which improves the processing capacity for the EMP of a heterogeneous energy system. As depicted in Figure 1, the structure of the seaport integrated energy system can be divided into the physical layer, energy management center, and data processing center, respectively.

Specifically, the physical layer integrates the production and consumption devices and monitors their operational states. Moreover, the physical layer transmits the relatable state information to the data processing center. According to the regional and autonomous features of the seaport integrated energy system, the data information can be split into the state of internal nodes and external nodes, respectively. As for the data processing center, it performs well on the full-dimensional definition of the physical structure and communication topology. Moreover, it supports various applications, which guarantees the flexibility and intelligence of the seaport integrated energy system during energy management. The energy management center focuses on analyzing the operational mechanisms of devices and constructing the energy management model of the seaport integrated energy system. It also majors on calculating the optimal solutions of the EMP with the designed intelligent energy management algorithm. Then, the optimal solutions will be transmitted to the data processing and physical layers simultaneously.

Based on the analysis above, the seaport integrated energy system can be commonly regarded as an efficient structure to realize the specific energy allocation suitable for the regional, sustainable, and complex seaport integrated energy system.

2.2. Energy Generation Device Modeling

Seaports have gradually become large-scale comprehensive multi-energy systems, mainly relying on power and coupling with other heterogeneous energy sources. To analyze the EMP conveniently, the mathematical operation models of conventional generators, renewable energy generators, energy storage devices, carbon capture, and carbon storage devices are demonstrated as follows [36–38].

(1) Conventional generators. The fuel-based power generators (FBPG), power-to-gas generators (P2G), fuel-based heating generators (FBHG), and gas producers (GP) are considered. Moreover, the consumption cost functions can be expressed as

$$\begin{aligned} &C_{\mathrm{FP}}(P_{\mathrm{FP}}) = a_{\mathrm{FP}}P_{\mathrm{FP}}^2 + b_{\mathrm{FP}}P_{\mathrm{FP}} + \gamma_{\mathrm{FP}} \\ &C_{\mathrm{P2G}}(P_{\mathrm{P2G}}) = a_{\mathrm{P2G}}b_{\mathrm{P2G}}P_{\mathrm{P2G}} \\ &C_{\mathrm{FH}}(h_{\mathrm{FH}}) = a_{\mathrm{FH}}h_{\mathrm{FH}}^2 + b_{\mathrm{FH}}h_{\mathrm{FH}} + \gamma_{\mathrm{FH}} \\ &C_{\mathrm{GP}}(g_{\mathrm{GP}}) = a_{\mathrm{GP}}g_{\mathrm{GP}}^3 + b_{\mathrm{GP}}g_{\mathrm{GP},i}^2 + \gamma_{\mathrm{GP}}g_{\mathrm{GP}} + \theta_{\mathrm{GP}} \\ &C_{\mathrm{CHP}}(P_{\mathrm{CHP}}, h_{\mathrm{CHP}}) \\ &= a_{\mathrm{CHP}}P_{\mathrm{CHP}}^2 + b_{\mathrm{CHP}}P_{\mathrm{CHP}} + \tilde{a}_{\mathrm{CHP}}h_{\mathrm{CHP}}^2 \\ &+ \tilde{b}_{\mathrm{CHP}}h_{\mathrm{CHP}} + \gamma_{\mathrm{CHP}}P_{\mathrm{CHP}}h_{\mathrm{CHP}} + \theta_{\mathrm{CHP}} \end{aligned} \tag{1}$$

where $C_{\mathrm{FP}}(\bullet)$, $C_{\mathrm{P2G}}(\bullet)$, $C_{\mathrm{FH}}(\bullet)$, $C_{\mathrm{GP}}(\bullet)$ and $C_{\mathrm{CHP}}(\bullet)$ are the consumption costs of FBPG, P2G, FBHG, GP, and CHPG, respectively. P_{FP}, g_{P2G}, h_{FH}, g_{GP}, P_{CHP}, and h_{CHP} are the energy outputs supplied by FBPG, P2G, FBHG, GP, and CHPG, respectively. $P_{\mathrm{P2G}} = (g_{\mathrm{P2G}} \cdot \delta_{\mathrm{SNG}})/\eta_{\mathrm{P2G}}$ denotes the relationship between the power and gas generation in P2G. δ_{SNG} is a constant higher heating value of synthetic natural gas (SNG). η_{P2G} is the exchange efficiency. a_{FP}, b_{FP}, γ_{FP}, a_{P2G}, b_{P2G}, a_{FH}, b_{FH}, γ_{FH}, a_{GP}, b_{GP}, γ_{GP}, θ_{GP}, a_{CHP}, b_{CHP}, $\tilde{a}_{\mathrm{CHP}}$, $\tilde{b}_{\mathrm{CHP}}$, γ_{CHP}, θ_{CHP} are the operation coefficients of FBPG, P2G, FBHG, GP, and CHPG respectively, depending on the devices themselves.

(2) Renewable generators and energy storage devices. Renewable power generator(s) (RPG) and renewable heating generator(s) (RHG) are considered in seaport integrated energy systems. Meanwhile, to decrease the fluctuation caused by renewable sources, power storage devices (PSD), and heating storage devices (HSD) are indispensable. The mathematics of the consumption costs are as follows

$$\begin{aligned} C(P_{\mathrm{RP}}) &= a_{\mathrm{RP}}P_{\mathrm{RP}} \\ &\quad + b_{\mathrm{RP}}\exp[r_{\mathrm{RP}}(\bar{P}_{\mathrm{RP}} - P_{\mathrm{RP}})/(\bar{P}_{\mathrm{RP}} - \tilde{P}_{\mathrm{RP}})] \\ C(h_{\mathrm{RH}}) &= a_{\mathrm{RH}}h_{\mathrm{RH}} \\ &\quad + b_{\mathrm{RH}}\exp[r_{\mathrm{RH}}(\bar{h}_{\mathrm{RH}} - h_{\mathrm{RH}})/(\bar{h}_{\mathrm{RH}} - \tilde{h}_{\mathrm{RH}})] \\ C(P_{\mathrm{PS}}) &= a_{\mathrm{PS}}(P_{\mathrm{PS}} + b_{\mathrm{PS}})^2 + \gamma_{\mathrm{PS}}|P_{\mathrm{PS}}| \\ C(h_{\mathrm{HS}}) &= a_{\mathrm{HS}}(h_{\mathrm{HS}} + b_{\mathrm{HS}})^2 + \gamma_{\mathrm{HS}}|h_{\mathrm{HS}}| \end{aligned} \tag{2}$$

where P_{RP}, h_{RH} are the power and heating outputs supplied by RPG and RHG, respectively. P_{PS} and h_{HS} are the power and heating charged/discharged values, respectively. $C_{\mathrm{RP}}(\bullet)$, $C_{\mathrm{RH}}(\bullet)$, $C_{\mathrm{PS}}(\bullet)$, $C_{\mathrm{HS}}(\bullet)$ are the consumption costs of RPG, RHG, PSD, and HSD, respectively. The cost parameters a_{RP}, b_{RP}, a_{RH}, b_{RH} are all nonnegative constants. The common penalty factors r_{RP} and r_{RH} are lower than zero. $(\tilde{\bullet})$ and $(\bar{\bullet})$ denote the lower and upper bound values, respectively. $|\bullet|$ denotes the absolute value. γ_{PS} and γ_{HS} are the consumption costs of the charging/discharging unit power and heating, respectively.

(3) Carbon capture and carbon storage devices. To reduce greenhouse emissions, it is necessary to delineate the operation costs of carbon dioxide. The consumption costs of the carbon capture (CA) and carbon storage devices both majorly depend on the carbon-absorbing mass, which is defined as

$$C_{\mathrm{CA}}(P, h, g) = a_{\mathrm{P}}E_{\mathrm{CO_2,P}} + a_{\mathrm{H}}E_{\mathrm{CO_2,H}} + a_{G}E_{\mathrm{CO_2,G}} \tag{3}$$

with

$$\begin{aligned} E_{\mathrm{CO_2,P}} &= \textstyle\sum_{i\in \mathrm{C_P}} b_{\mathrm{P},i}\theta_{\mathrm{P},i}P_i \\ E_{\mathrm{CO_2,H}} &= \textstyle\sum_{i\in \mathrm{C_H}} b_{\mathrm{H},i}\theta_{\mathrm{H},i}h_i \\ E_{\mathrm{CO_2,G}} &= \textstyle\sum_{i\in \mathrm{C_G}} b_{\mathrm{G},i}\theta_{\mathrm{G},i}g_i \end{aligned} \tag{4}$$

where $C_{CA}(\bullet)$ is the carbon-absorbing cost of the multi-energy generators. $E_{CO_2,P}$, $E_{CO_2,H}$, and $E_{CO_2,G}$ are the carbon-absorbing masses from fuel-based generators of power, heating, and gas networks, respectively. a_P, a_H, and a_G are the operation costs of absorbing unit carbon emissions from the fuel-based generators of power, heating, and gas networks, respectively. b_P, b_H, and b_G are the capturing unit carbon emission efficiencies from the power, heating, and gas networks, respectively. θ_P, θ_H, and θ_G are the carbon emission efficiencies of fuel-based generators of power, heating, and gas networks, respectively. Specifically, the masses of carbon exhausted, containing $\tilde{E}_{CO_2,P}$, $\tilde{E}_{CO_2,H}$, and $\tilde{E}_{CO_2,G}$, are expressed as

$$\begin{aligned} \tilde{E}_{CO_2,P} &= \sum_{i \in C_P} (1 - b_{P,i}) \theta_{P,i} P_i \\ \tilde{E}_{CO_2,H} &= \sum_{i \in C_H} (1 - b_{H,i}) \theta_{H,i} h_i \\ \tilde{E}_{CO_2,G} &= \sum_{i \in C_G} (1 - b_{G,i}) \theta_{G,i} g_i \end{aligned} \tag{5}$$

Meanwhile, since carbon capture devices and carbon storage devices consume power in the operation state, they can also be regarded as load devices. Moreover, the relationship between power consumption and carbon emissions can be expressed as

$$\begin{aligned} P_{Ca} &= P_{Ca,fixed} + \psi_{Ca,P}(E_{CO_2,P} + E_{CO_2,H} + E_{CO_2,G}) \\ P_{St} &= r_{St,P}(E_{CO_2,P} + E_{CO_2,H} + E_{CO_2,G}) \end{aligned} \tag{6}$$

where P_{Ca} and P_{St} involve the power consumption of carbon capture devices and carbon storage devices, respectively. $P_{Ca,fixed}$ is the fixed operating cost, which is positively associated with power consumption. $\psi_{Ca,P}$ represents the power consumption efficiency of the carbon capture unit, while $r_{St,P}$ represents the power consumption efficiency of the carbon storage unit.

(4) Energy load devices. The benefits of revenue functions of the power load devices (PL), heating load devices (HL), and gas load devices (GL) can be commonly viewed as convex quadratic functions, which can be defined as

$$\begin{aligned} U_i^P &= a_i^P P_i^2 + b_i^P P_i + \gamma_i^P \\ U_i^H &= a_i^H h_i^2 + b_i^H h_i + \gamma_i^H \\ U_i^G &= a_i^G g_i^2 + b_i^G g_i + \gamma_i^G \end{aligned} \tag{7}$$

where P_i, h_i, and g_i are the power, heating, and gas load demands at the ith node, respectively. a_i^P, b_i^P, γ_i^P, a_i^H, b_i^H,γ_i^H, a_i^G, b_i^G, and γ_i^G are the constant coefficients.

2.3. Multi-Energy Network Constraints

The supply–demand balance and energy output constraints should be concerned to ensure the reliable operation of the seaport integrated energy system.

(1) Supply–demand balance constraints. The power, heating, and gas supply–demand balance constraints can be denoted as

$$\begin{aligned} \sum_{z_i \in \Omega_{In}^z} P_{z_i} + \sum_{z_i \in \Omega_{Ex}^z} P_{z_i} - P_{Ca} - P_{St} &= P_L \\ \sum_{z_i \in \Omega_{In}^z} h_{z_i} + \sum_{z_i \in \Omega_{Ex}^z} h_{z_i} &= h_L \\ \sum_{z_i \in \Omega_{In}^z} g_{z_i} + \sum_{z_i \in \Omega_{Ex}^z} g_{z_i} &= g_L \end{aligned} \tag{8}$$

where P_L, h_L, and g_L are the total power, heating, and gas load demands of m energy bodies in the seaport integrated energy system, respectively. For $\forall z \in \Omega_m$, Ω_{In}^z and Ω_{Ex}^z denote the internal nodes and external nodes of the zth EB, respectively. $\Omega_{In}^z = C_P^z \cup C_H^z \cup C_G^z$, and $\Omega_{Ex}^z = C_P^{z'} \cup C_H^{z'} \cup C_G^{z'}$, where $z \in \{1, 2, .., m\}$ and $z' \in \{1, 2, ..., z-1, z+1, ..., m\}$. Moreover, $\Omega_{In}^z \cup \Omega_{Ex}^z = C$ is satisfied.

(2) Energy output constraints. In order to ensure the secure operation of generators, energy outputs constraints are needed, which can be expressed as

$$\tilde{P} \preceq P \preceq \bar{P}, \tilde{h} \preceq h \preceq \bar{h}, \tilde{g} \preceq g \preceq \bar{g} \tag{9}$$

where $P = [P_{\mathrm{FD}}, P_{\mathrm{CHP}}, P_{\mathrm{RP}}, P_{\mathrm{PS}}, P_{\mathrm{P2G}}]^{\mathrm{T}}$ is the compact set of power outputs. The compact set of heating outputs is denoted as $h = [h_{\mathrm{FH}}, h_{\mathrm{CHP}}, h_{\mathrm{RH}}, h_{\mathrm{HS}}]^{\mathrm{T}}$. $g = [g_{\mathrm{GP}}, g_{\mathrm{P2G}}]^{\mathrm{T}}$ is the compact set of gas outputs.

2.4. Multi-Objective Seaport Energy Management

The energy management of the seaport integrated energy system primarily focuses on the combined effects of consumption costs, greenhouse gas emissions, and carbon trading. The mathematical expression is as follows

$$\min\{F_{\mathrm{OP}}, F_{\mathrm{GE}}, F_{\mathrm{CT}}\} \tag{10}$$

where F_{OP} is the total consumption cost of the seaport integrated energy system. F_{OP} is the total mass of greenhouse gas emissions. F_{CT} is the total carbon trading cost, which depends on the surplus carbon unabsorbed by the carbon capture device and the carbon tax price.

(1) Economic objective function. The total consumption cost F_{OP} is related to the benefit revenues of the load devices and the operation costs of generators, shown as

$$F_{\mathrm{OP}} = \sum_{z_i \in \Omega^{\mathrm{z}}_{\mathrm{In}}} (C_{z_i} - U_{z_i}) + \sum_{{z'}_i \in \Omega^{\mathrm{z}}_{\mathrm{Ex}}} (C_{{z'}_i} - U_{{z'}_i}) \tag{11}$$

where C_{z_i} and U_{z_i} are the operation cost and revenue benefit of the z_ith node, respectively.

(2) Environmental objective function. To reduce gas pollution, such as $\mathrm{NO_X}$ and $\mathrm{SO_X}$, the emission mass of the seaport integrated energy system should be considered, which is defined as

$$\begin{aligned} F_{\mathrm{GE}} = &\textstyle\sum_{z_i \in \Omega^{\mathrm{z}}_{\mathrm{In}}} [E_{\mathrm{P}}(P_{z_i}) + E_{\mathrm{H}}(h_{z_i}) + E_{\mathrm{G}}(g_{z_i})] \\ &+ \textstyle\sum_{z'_i \in \Omega^{\mathrm{z}}_{\mathrm{Ex}}} [E_{\mathrm{P}}(P_{z'_i}) + E_{\mathrm{H}}(h_{z'_i}) + E_{\mathrm{G}}(g_{z'_i})] \end{aligned} \tag{12}$$

where $E_{\mathrm{P}}(P) = s_{\mathrm{P}}P^2 + v_{\mathrm{P}}P + c_{\mathrm{P}} + t_{\mathrm{P}}e^{\tau P}$, $E_{\mathrm{H}}(h) = (c_{\mathrm{H}} + v_{\mathrm{H}})h$, and $E_{\mathrm{G}}(g) = (c_{\mathrm{G}} + v_{\mathrm{G}})g$ are the gas pollutions generated by power, heating, and gas generation devices, respectively. Moreover, the emission expression of CHP is defined as $E_{\mathrm{CHP}}(P_{\mathrm{CHP}}) = (c_{\mathrm{CHP}} + v_{\mathrm{CHP}})P_{\mathrm{CHP}}$. s_{P}, v_{P}, v_{H}, v_{G}, c_{P}, c_{H}, c_{G}, t_{P}, and τ_{P} are the emission coefficients of the energy generation devices, respectively.

(3) Carbon trading objective function. In order to increase the absorption mass of carbon, namely by reducing carbon exhaustion, carbon trading is a necessary focus, which can be expressed as

$$F_{\mathrm{CT}} = C_{\mathrm{CA}} + \sigma_{\mathrm{Tax}}(\tilde{E}_{\mathrm{CO_2,P}} + \tilde{E}_{\mathrm{CO_2,H}} + \tilde{E}_{\mathrm{CO_2,G}}) \tag{13}$$

where σ_{Tax} is the carbon tax price, namely the trading price of an emitting unit mass of carbon.

3. Distributed Seaport Energy Management Strategy

3.1. Preliminaries

Let $\mathcal{G} = (\mathcal{V}, \mathcal{E}, \mathcal{A})$ denote the undirected communication topology of the seaport integrated energy system, where $\mathcal{V} = \mathcal{V}_{\mathrm{P}} \cup \mathcal{V}_{\mathrm{H}} \cup \mathcal{V}_{\mathrm{G}}$, $\mathcal{E} = \mathcal{V} \times \mathcal{V}$, and $\mathcal{A} = \{a_{z_i,z_j} | z_i, z_j \in \mathrm{C}\}$ are the node set, communication information edge set, and adjacency matrix, respectively. To be specific, when node v_{z_i} and v_{z_j} are both in $\mathcal{E}$, we have $a_{z_i,z_j} = 1$, where the z_ith node and the z_jth node can exchange state information with each other. Otherwise, $a_{z_i,z_j} = a_{z_j,z_i} = 0$, which means that node v_{z_i} and v_{z_j} cannot exchange operation states with each other. Meanwhile, for the zth EB, there are $n_z = n_z^{\mathrm{p}} + n_z^{\mathrm{h}} + n_z^{\mathrm{g}}$ nodes in the internal node

set Ω_{In}^{z}, and $|\text{C}| - n_z = (n_1 + ... + n_{z-1} + n_{z+1}, ..., n_m)$ nodes in the external node set Ω_{Ex}^{z}, respectively.

The analysis mentioned above shows that the economic, environmental, and carbon trading objectives in (10) all perform the convex features. Considering the contradictions between the multi-objectives, it is necessary to resolve the relationships between F_{OP}, F_{GE}, and F_{OP}. A dynamic-weighted coefficient set $\mathbf{!} = [\alpha, \beta, \alpha]$ is designed here to reconstruct the seaport multi-objective EMP as a single goal–optimal problem concerning the three objectives simultaneously, which can be expressed as

$$\min\{\alpha F_{\text{OP}} + \beta F_{\text{GE}} + \alpha F_{\text{CT}}\} \tag{14}$$

Remark 1. *The economic objective F_{OP} and the carbon trading objective F_{CT} for the seaport energy management have the same unit. Unlike the other objectives, the unit of environmental objective F_{GE} is the gas emission mass. Therefore, the weighted coefficient of F_{GE} is different from F_{OP} and F_{CT}.*

Then, the EMP of the seaport integrated energy system is constructed by (11)–(14), which is a commonly convex optimization problem with the decision variable Y, namely

$$Y = [\underbrace{(\boldsymbol{y}_1^p)^{\text{T}}, (\boldsymbol{y}_1^h)^{\text{T}}, (\boldsymbol{y}_1^g)^{\text{T}}}_{1-st\text{EB}}, ..., \underbrace{(\boldsymbol{y}_m^p)^{\text{T}}, (\boldsymbol{y}_m^h)^{\text{T}}, (\boldsymbol{y}_m^g)^{\text{T}}}_{m-\text{thEB}}]^{\text{T}}$$

where $\boldsymbol{y}_z^p = [P_{z_1}, ..., P_{z_{n_z}}]^{\text{T}}$, $\boldsymbol{y}_z^h = [h_{z_1}, ..., h_{z_{n_z}}]^{\text{T}}$, $\boldsymbol{y}_z^g = [g_{z_1}, ..., g_{z_{n_z}}]^{\text{T}}$. Then, the compact mathematical expression of the EMP can be constructed as

$$\begin{aligned} &\min f(Y) = \mathscr{F}(\mathscr{A}_{\text{P}} Y) + \mathscr{F}(\mathscr{A}_{\text{H}} Y) + \mathscr{F}(\mathscr{A}_{\text{G}} Y) \\ &s.t. \sum\nolimits_{z_i \in \Omega_{\text{In}}^{z}} A_{z_i} y_{z_i} + \sum\nolimits_{z_i' \in \Omega_{\text{Ex}}^{z}} A_{z_i'} y_{z_i'} = \boldsymbol{b} \end{aligned} \tag{15}$$

where $\mathscr{A}_{\text{P}}$, $\mathscr{A}_{\text{H}}$, and $\mathscr{A}_{\text{G}}$ are the conversion coefficients of "1" and "0", which can extract the needed variables from Y. $\boldsymbol{b}$ is a constant vector; each element can be calculated and obtained by the given topology structure.

3.2. Main Algorithm

Considering the self-sufficiency features of the seaport integrated energy system-based EB, this section focuses on designing a fully distributed strategy based on the multi-agent system theory and the event-triggered communication mechanism to solve the EMP (15) against the bandwidth limitation of the seaport.

Firstly, let $t_{z_i}^k$ denote the latest event-triggered time of the z_ith node, the z_jth node is the neighbor of the z_ith node, and k is the event instant of the z_ith node. Meanwhile, the measurement error is defined as

$$e_{z_i} = \hat{\lambda}_{z_i}(t_{z_i}^k) - \lambda_{z_i}(t), \forall t \in [t_{z_i}^k, t_{z_i}^{k+1}), \forall z_i \in \text{C} \tag{16}$$

where $\lambda = [\boldsymbol{\lambda}_1^{\text{T}}, ..., \boldsymbol{\lambda}_m^{\text{T}}]^{\text{T}}$ is the Lagrange multiplier, which is noted as the incremental cost vector of the power, heating, and gas at each node in the m energy bodies, and $\boldsymbol{\lambda}_z = [\lambda_{z_1}, ..., \lambda_{z_{n_z}}]^{\text{T}}$. $\hat{\lambda}_{z_i}$ and $\hat{\lambda}_{z_j}$ are the incremental costs of the z_ith node and the z_jth node at the latest triggering time. Then, a fully distributed energy management strategy is proposed in **Algorithm 1**.

Algorithm 1: Seaport energy management strategy.

Input: The information communication topology and physical structure of the seaport integrated energy system $\mathcal{G} = (\mathcal{V}, \mathcal{E}, \mathcal{A})$. We set the initial values of λ_0 and Y_0.

for The z_ith node of the zth EB, where $z_i \in \mathrm{C}$, $z \in \Omega_{\mathrm{m}}$, **do**

  Detection and judgment.

  Set $\mathcal{X}_{z_i} = \eth_{z_i}(t^k_{z_i}) e^2_{z_i}(t^k_{z_i})$, where $\eth_{z_i}$ is a custom variable, which is presented in Appendix-A, (A-1).

  if $\mathcal{X}_{z_i} = 0$ and $e^2_{z_i}(t^k_{z_i}) \neq 0$, for $\forall t \in [t^k_{z_i}, +\infty)$, **then**

    broad is the state of $\hat{\lambda}_{z_i}(t^k_{z_i})$. **We update** the control protocol state

    $\dot{\lambda}_{z_i}(t) = -2qc_{z_i}[\sum_{z_j \in \Omega^z_{\mathrm{In}}} a_{z_i,z_j}(\hat{\lambda}_{z_i}(t^k_{z_i}) - \hat{\lambda}_{z_j}(t^{k'}_{z_j}))$

    $+ \sum_{z_j \in \Omega^z_{\mathrm{Ex}}} a_{z_i,z_j}(\hat{\lambda}_{z_i}(t^k_{z_i}) - \hat{\lambda}_{z_j}(t^{k'}_{z_j}))]$

    where q is an adjustable control parameter. c_{z_i} is the energy participant's operation coefficient of the z_ith node.

    Output: the values of $\lambda_{z_i}(t^k_{z_i})$, e_{z_i}, and $t^k_{z_i}$.

  else

    We update the auxiliary variable $\mathcal{X}_{z_i}$, where

    $\mathcal{X}_{z_i}(t) = \eth_{z_i}(t)[\lambda_{z_i}(t^k_{z_i}) - \lambda_{z_i}(t)]^2$. **Return** 4.

Assumption 1. *The communication between the energy bodies of the seaport integrated energy system is undirected. Moreover, we assume that the EMP (15) is solvable, which means that at least one seaport energy management solution can be acquired to meet all of the physical constraints under (15).*

With the **Assumption 1** and **Algorithm 1**, two theorems can be deduced.

Theorem 1. *For the EMP of the seaport integrated energy system (15), in the optimal distributed strategy with the event-triggered mechanism proposed in **Algorithm 1**, there exists a positive minimal inter-event time $\mathcal{T}_{z_i}$ at the ith node of the zth EB, which satisfies $t^{k+1}_{z_i} - t^k_{z_i} \geq \mathcal{T}_{z_i}$, where t^{k+1} and t^k are the kth and $(k+1)$th triggering times, respectively.*

Proof. The proof is demonstrated in Appendix A.1. □

Theorem 2. *The incremental costs of power, heating, and gas can converge to the optimal energy management solution of (15) by the proposed distributed strategy with the event-triggered condition (ETC), namely*

$$t^{k+1}_{z_i} := \left\{ t \middle| \eth_{z_i}(t^k_{z_i}) e^2_{z_i}(t^k_{z_i}) = 0, e_{z_i}(t^k_{z_i}) \neq 0, t > t^k_{z_i} \right\} \tag{17}$$

Proof. The convergence is proved in Appendix A.2. □

According to the analysis above, the proposed distributed seaport energy management strategy can realize collaborative energy allocation. Under **Algorithm 1**, it can be proved that the designed **ETC** (17) can avoid the infinite number of updates to the auxiliary variable $\mathcal{X}$ in a finite time. Namely, the communication mechanisms among the energy bodies of the seaport integrated energy system refrain from the Zeno phenomena. To this end, the bandwidth limitation condition of the seaport can be tolerant with the designed distributed seaport optimal strategy-based event-triggered mechanism.

4. Simulation Results

Assume that the tested seaport integrated energy system contains 33 nodes with 6 energy bodies, including 17 energy generation nodes, 2 energy storage nodes, and 14 pure load nodes, whose basic physical structures and communication topologies are depicted in Figure 2. Specifically, EBs 1–6 contain [6, 6, 5, 5, 6, 5] nodes, respectively. Each EB can only

exchange the state information with its adjacent energy body, and the state information of the internal nodes in the same EB can exchange with each other. From Figure 2, it is obvious that the communication topology is undirected and connected. The operation parameters and the gas emission coefficients are listed in Tables 1 and 2, respectively. Moreover, the weighted coefficients are set as ω = [0.4, 0.2, 0.4]. Denote the energy consumption coefficients of capturing the unit carbon as $\theta_P = \theta_H = \theta_G = 0.7$. We unify the energy scales of the power, heating, and gas networks. Specifically, for the power and heating networks, 1 p.u. = 1 MW, for the gas network, 1 p.u. = 84SCM/h, and for the unit price, 1 p.u. = 1$/MWh.

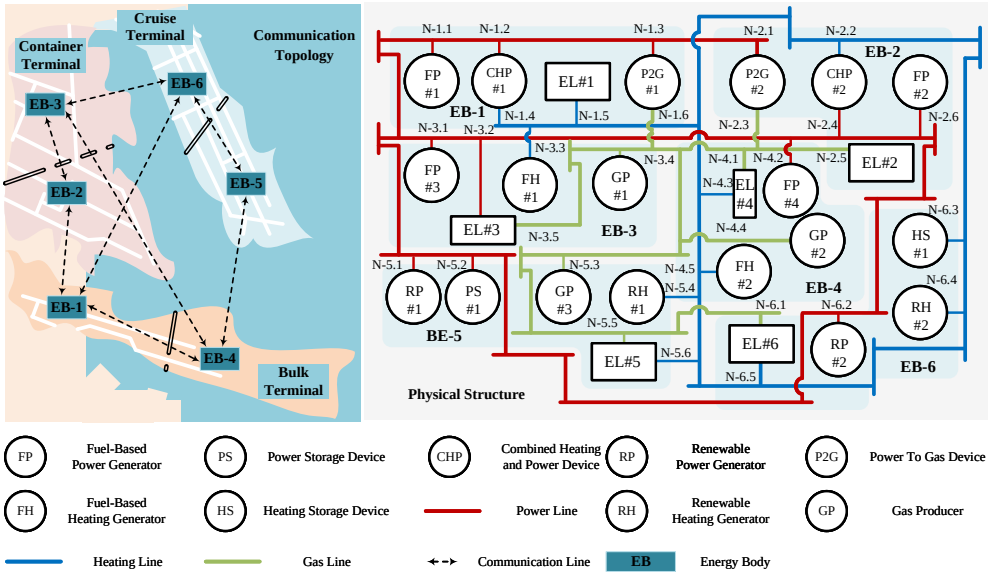

Figure 2. Structure of the tested seaport integrated energy system.

Table 1. Operation parameters of the tested system.

Category	a	b	$\tilde{a}$	$\tilde{b}$	r	θ	ψ	min	max
FP-1	0.3500	2.85	–	–	32	–	0.98	50	220
FP-2	0.3920	2.65	–	–	28	–	0.98	50	220
FP-3	0.4200	2.35	–	–	25	–	0.98	50	220
FP-4	0.3380	2.55	–	–	24	–	0.98	50	220
CHP-1	0.0345	12.50	0.03	4.2	0.031	230	0.98	50	220
CHP-2	0.0362	12.30	0.027	3.8	0.025	124	0.98	50	220
RP-1	0.1200	310	–	–	−1.2	–	0.98	90	120
RP-2	0.1500	285	–	–	−1.2	–	0.98	80	110
PS-1	0.4300	0.08	–	–	0.058	–	0.98	−50	70
PL	0.0050	2.60	–	–	60	–	–	50	800
FH-1	0.1000	4.55	–	–	100	–	0.98	45	100
FH-2	0.1200	4.35	–	–	100	–	0.98	45	100
RH-1	0.0650	350	–	–	−1.2	–	0.98	50	150
RH-2	0.0720	365	–	–	−1.2	–	0.98	50	150
HS-1	0.4400	0.09	–	–	0.058	–	0.98	−40	60

Table 1. *Cont.*

Category	a	b	$\tilde{a}$	$\tilde{b}$	r	θ	ψ	min	max
HL	0.0040	5.60	–	–	40		–	50	800
P2G-1	0.0300	100	–	–	–	–	0.98	50	150
P2G-2	0.0500	75	–	–	–	–	0.98	50	150
GP-1	2×10^{-6}	0.006	–	–	50	5	0.98	100	1000
GP-2	3×10^{-6}	0.003	–	–	35	6	0.98	100	1000
GP-3	4×10^{-6}	0.001	–	–	30	3	0.98	100	1000
GL	0.0040	4.60	–	–	75	–	–	50	800

Table 2. Emission coefficients of the tested system.

Category	a	b	c	v	s	t	τ
FP	1.0	0.85	0.041	−2.7	0.649	2	0.03
FH	1.0	0.90	0.00050	0.0080	–	–	–
GP	1.0	0.88	0.00055	0.0075	–	–	–
CHP	–	–	0.00015	0.0015	–	–	–
CA	$\psi_{\mathrm{Ca,P}} = 0.64$			ST	$r_{\mathrm{St,P}} = 4.89$		

4.1. Case Study A: Effectiveness Test

This section focuses on verifying the effectiveness of the proposed distributed seaport energy management strategy. Moreover, consumption costs, greenhouse gas emissions, and carbon trading are concentrated. Set the load demands of the seaport integrated energy system as [750, 640, 660] (p.u.) for the power, heating, and gas networks, respectively.

By applying the distributed energy management strategy proposed in **Algorithm 1**, the simulation solutions can be obtained, whose iteration trajectories of power, heating, and gas are depicted in Figure 3. The corresponding energy generations and load demands for each EB can still converge to stable values within 70 iteration steps. Moreover, the power, heating, and gas network's final incremental costs are [0.1697, 0.1104, 0.1455] (p.u.), respectively. The global energy load demands can be satisfied, which also ensure the energy output constraints. Meanwhile, the results of the consumption costs, NO_X/SO_X, gas emissions, and carbon trading are [16,193.8317, 420.8041, 14,762.8969], respectively. The specified optimal energy management solutions acquired by the conventional centralized strategy without the event-triggered mechanism and the proposed distributed algorithm under the consideration of the event-triggered mechanism are listed in Table 3. The final optimal solutions are almost the same. Most errors between solutions obtained by the two strategies are lower than 2.2 MW. There are just four nodes whose generation/consumption of energy exceeds 20 MW. The analysis mentioned above implies the effectiveness of the proposed distributed seaport energy management strategy for the seaport integrated energy system.

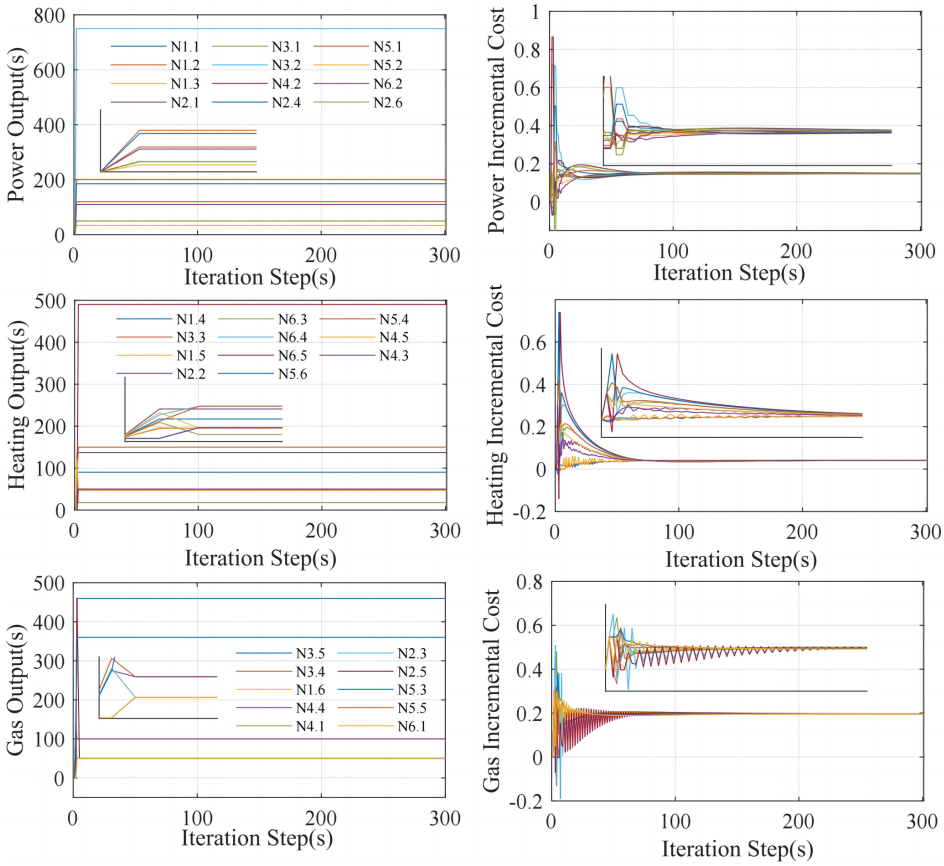

Figure 3. Energy generations and incremental costs of the test system.

Table 3. Energy output/load demand results between two strategies.

	Num	Category	Distributed	Centralized	Error
EB-1	N-1.1	FP-1	50.0000	50.0000	0.0000
	N-1.2	CHP(P)-1	200.4699	220.0000	0.4700
	N-1.3	P2G(P)-1	50.0000	50.0000	0.0000
	N-1.4	CHP(h)-1	89.9844	131.0221	41.0400
	N-1.5	EL(h)-1	46.9312	50.0000	0.0700
	N-1.6	P2G(g)-1	50.0000	50.0000	0.0000
EB-2	N-2.1	P2G(P)-2	50.0000	50.0000	0.0000
	N-2.2	CHP(h)-2	136.7656	109.6480	27.1200
	N-2.3	P2G(g)-2	50.0000	50.0000	0.0000
	N-2.4	CHP(P)-2	185.1220	129.7857	55.3360
	N-2.5	EL(g)-2	50.0000	50.0002	0.0002
	N-2.6	FP-2	50.0000	50.0000	0.0000
EB-3	N-3.1	FP-3	50.0000	50.0001	0.0001
	N-3.2	EL(P)-3	750.0000	750.0000	0.0000
	N-3.3	FH-1	46.9312	45.0000	1.9310
	N-3.4	GP-1	100.0000	100.0000	0.0000
	N-3.5	EL(g)-3	50.0000	50.0001	0.0001
EB-4	N-4.1	EL(g)-4	50.0000	50.0000	0.0000
	N-4.2	FP-4	50.0000	50.2145	0.2145
	N-4.3	EL(h)-4	50.0000	50.0000	0.0000
	N-4.4	GP-2	100.0000	100.0000	0.0000
	N-4.5	FH-2	47.7852	45.0000	2.7852

Table 3. *Cont.*

	Num	Category	Distributed	Centralized	Error
EB-5	N-5.1	RP-1	120.0000	120.0000	0.0000
	N-5.2	PS-1	34.4081	69.9997	35.5920
	N-5.3	GP-3	360.0000	359.9999	0.0001
	N-5.4	RH-1	150.0000	141.5222	8.4780
	N-5.5	EL(g)-5	50.0000	50.0000	0.0000
	N-5.6	EL(h)-5	50.0000	50.0000	0.0000
EB-6	N-6.1	EL(g)-6	460.0000	459.9997	0.0003
	N-6.2	RP-2	110.0000	110.0000	0.0000
	N-6.3	HS-1	18.5346	17.8186	0.7160
	N-6.4	RH-2	150.0000	149.9892	0.0108
	N-6.5	EL(h)-6	490.0000	490.0000	0.0000

4.2. Case Study B: Multi-Objectives Results Analysis

This section tests the capacity to reduce communication resources by applying the proposed distributed strategy with the event-triggered mechanism instead of the peer-to-peer communication mechanism. Moreover, the comprehensive assessment values of the multi-objective energy management were analyzed. All of the initial conditions are the same as **Case Study A**.

With the proposed distributed energy management strategy, the communication pattern among energy entities operates discretely. The energy participant can be triggered with the effect of **ECT** designed in (17). The event-triggered instants of energy management are depicted in Figure 4, showing the trigger moment from 7 nodes in 4 energy bodies. From Figure 4, the maximal inter-event time is 13 iteration steps (the 199th to 214th iteration steps), which happens in node N5.3. Unlike the proposed strategy, the traditional energy management strategy without an event-triggered mechanism depends on real-time and continuous communication. To this end, the total number of communication iteration times in Figure 4 can be saved by more than 2100 times, verifying that the proposed strategy needs fewer communication resources than the conventional communication mechanism. Therefore, it is worth noting that the proposed distributed energy management strategy is suitable for the seaport integrated energy system under the limited communication bandwidth.

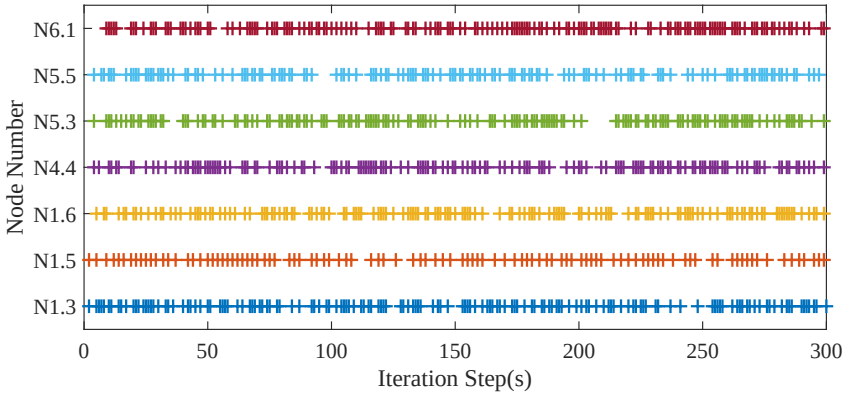

Figure 4. Time evolution of event-triggered instants.

Moreover, four scenarios were considered for testing the effectiveness of the seaport's multi-objective energy management model. Scenario 1 considers the economic, environmental, and carbon trading objectives simultaneously, which is the constructed energy management model (15). Scenario 2 takes the operation cost and carbon trading into consideration. Scenario 3 concerns the operation costs and gas emissions. Scenario 4 considers the gas emissions and carbon trading. At the moment, the dynamically weighted coefficient

sets of scenarios 1–4 are [0.4, 0.2, 0.4], [0.5, 0, 0.5], [0.5, 0.5, 0], [0, 0.5, 0.5], respectively. Table 4 lists the four optimal energy management solutions of the scenarios.

Table 4. Results of the comparison scenarios.

	Operation Cost	Gas Emission	Carbon Trading
Scenario 1	76,402.05074	40,313.05257	11,207.48219
Scenario 2	76,401.95006	161,192.7589	11,207.53908
Scenario 3	75,458.00884	40,313.34921	12,790.8009
Scenario 4	77,495.14439	40,106.19069	10,411.22709

As shown in Table 4, the carbon trading value of scenario 3 is higher than scenario 1. Moreover, the operation cost value of scenario 4 is higher than scenario 1. Moreover, the comprehensive evaluation results of scenarios 1–4 are [127,922.5855, 248,802.2481, 128,562.1589, 128,012.5622], whose detailed energy management solutions are shown in Figure 5. It is worth noting that the best performance is obtained by scenario 1 with minimal evaluation scores. Therefore, based on the analysis before, the proposed seaport multi-objective energy management model is more suitable for the seaport integrated energy system. Additionally, it satisfies the prospects of sustainable marine development with lower pollution emissions, advocated by IMO.

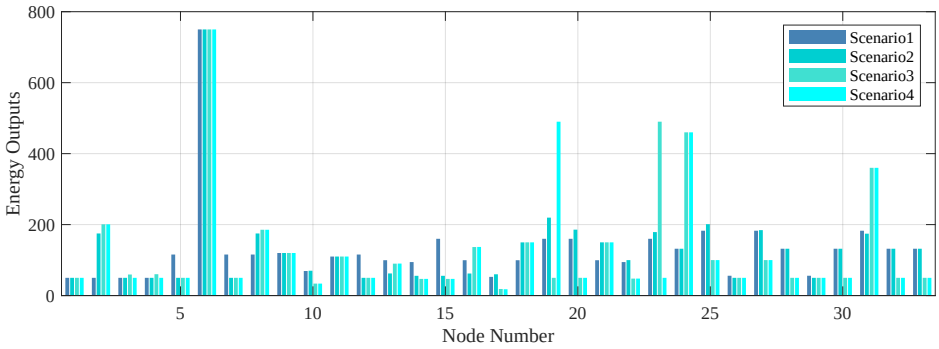

Figure 5. Energy outputs of 33 nodes.

4.3. Case Study C: Dynamically Weighted Coefficient Adjustment

This section tests the seaport's comprehensive evaluation property by adjusting the dynamic-weighted coefficients. The step sizes of the weighted coefficient of the consumption cost and carbon trading are 0.05. The step size of the weighted coefficient of gas emission is 0.1. By implementing the proposed seaport distributed optimal strategy in **Algorithm 1** with different dynamic-weighted coefficient sets, the simulation results are depicted in Figure 6.

Specifically, based on the same initial conditions, Figure 6 shows the evaluation results of multiple objectives under 11 sets of dynamic-weighted coefficients. The consumption costs of the seaport integrated energy system are calculated as [77,537.6890, 76,403.4451, 76,402.5181, 76,402.8514, 76,360.7091, 76,402.4295, 76,360.4674, 76,360.3516, 76,402.0507, 75,376.8047, 76,401.9501], respectively. The carbon trading costs are [10,417.2401, 11,204.3797, 11,206.3978, 11,206.8865, 11,207.1114, 11,207.2643, 11,207.3571, 11,207.4295, 11,207.4822, 11,207.5194, 11,207.5391], respectively. The results of carbon trading are much lower than the consumption costs and gas emissions. Moreover, Figure 7 shows the trajectory of the comprehensive evaluation results of the seaport's multiple-objective energy management under the dynamic-weighted coefficient sets. The comprehensive evaluation value decreases before the tenth dynamic-weighted coefficient set and rises sharply at the eleventh coefficient set. The minimal comprehensive evaluation result 126,897.3815 occurred in the tenth iteration with the weighted coefficient set [0.45, 0.10, 0.45]. Therefore, it can be

suggested that the most suitable weighted coefficients of (14) under the tested seaport integrated energy system are $\alpha = 0.45$, $\beta = 0.10$.

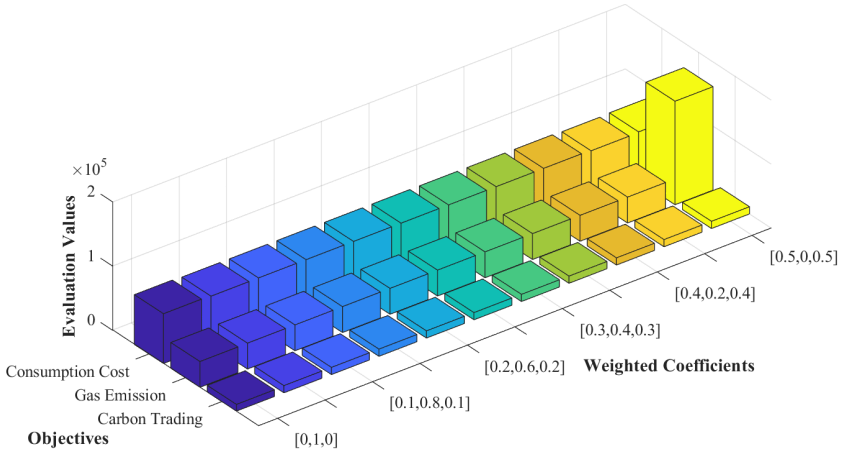

Figure 6. Evaluation values under dynamic-weighted coefficient sets.

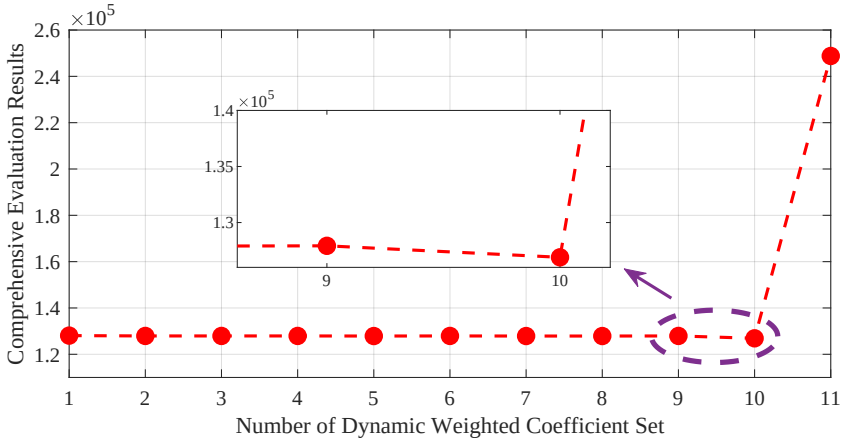

Figure 7. Comprehensive evaluation results.

According to the analysis above, the effectiveness of the proposed seaport-distributed energy management strategy in **Algorithm 1** is proved. The distributed strategy can effectively save communication resources between energy bodies, adaptable to the seaport's communication bandwidth limitations. Moreover, gas emissions and carbon trading are considered along with the consumption costs during the seaport's energy management. Furthermore, the most appropriate weighted coefficient set can be acquired.

4.4. Discussion on the Case Study Results

Optimal energy management solution. From Figure 3, the energy output/consumption and the incremental costs of energy devices from power, heating, and gas networks can rapidly converge to stable values with the proposed distributed energy management strategy. Furthermore, the comparisons of the detailed optimal solutions (between the distributed and centralized) are listed in Table 3. From the above analysis, most errors between the two solutions are less than 2.2 MW, which proves the accuracy of the designed distributed strategy. The energy management model constructed focuses on the operation costs, greenhouse gas emissions, and carbon trading, and the detailed results of each objective are [16,193.8317, 420.8041, 14,762.8969]. It is obvious that the operation cost is the most crucial factor in the seaport integrated energy system.

Moreover, the communication resource is sharply decreased by utilizing the proposed event-triggered mechanism between the energy bodies. We took seven nodes of the

tested system as an example. Figure 6 shows their communication states. The dots in Figure 6 describe the triggering times of the seven nodes. It suggests that each node can achieve convergence without successive communication with the adjacent neighbor node. Furthermore, during the blank time, the node keeps the previous state until the state is updated in the next triggering time.

From the case study results, it is worth noting that the proposed energy management strategy of the seaport integrated energy system in a distributed manner based on the event-triggered mechanism performs well at decreasing carbon emissions with fewer communication resources. This phenomenon manifests the sustainable development of the international shipping industry.

5. Conclusions

The distributed energy management strategy-based event-triggered communication mechanism is proven to greatly affect the multi-objective energy management problem with the goals of economic and environmental benefits for the seaport. Moreover, the rigorous theoretical derivation and the simulations based on a 33-node test system were utilized to verify the validity of the proposed method. The main conclusions are demonstrated in the following.

At first, the multi-objective energy management model of the seaport integrated energy system was constructed with dynamic-weighted coefficients, which considered greenhouse gas emissions, carbon trading, and operation costs. Next, with the aid of the event-triggered mechanism, the communication limitation problem of the seaport can be handled. The comparison results denote the accuracy of the proposed distributed energy management strategy. By considering carbon emissions, the multi-objective energy management strategy will have 48.59% lower greenhouse gas emissions than the conventional energy management pattern without carbon emissions and carbon trading. Moreover, the designed strategy is effective at reducing communication resources, which will have 2100 times lower than the successive communication between energy bodies.

However, the designed energy management model of the seaport integrated system ignores volatility and fluctuation caused by the energy generation of renewable energy generators, which will negatively impact the accuracy of the optimal energy management solution. To this end, the influences of uncertainties caused by weather, noise, etc., will be further concentrated on in the future.

Author Contributions: Conceptualization, validation, writing—original draft Y.Z.; methodology and formal analysis, Q.S.; supervision, Y.X. and T.L.; writing—review and editing, Y.X. and T.L.; funding acquisition, Q.S. and T.L. All authors have read and agreed to the published version of the manuscript.

Funding: This work is partially supported by the National Natural Science Foundation of China (Key Program) under grant 51939001 and partially by the National Natural Science Foundation of China under grant 52201407 and grant 61976033.

Institutional Review Board Statement: Not applicable.

Informed Consent Statement: Not applicable.

Data Availability Statement: Not applicable.

Conflicts of Interest: The authors declare no conflict of interest.

Appendix A

Appendix A.1. Proof of Theorem 1

To analyze the positive minimal release time between trigger times, $t_{z_i}^{k+1}$ and $t_{z_i}^{k}$, an auxiliary variable is defined as follows:

$$\varsigma e_{z_i}^2 = \chi_{z_i} \tag{A1}$$

Assume that $\delta_{z_i} = \mathcal{X}_{z_i} = 0$ when $t = t_{z_i}^k$, and increases to $\tilde{\delta}_{z_i}$ before $t = t_{z_i}^{k+1}$. Meanwhile, the interval time $t_{z_i}^{k+1} - t_{z_i}^k$ is equal to the time slot of the changes from $\tilde{\delta}_{z_i}$ to zero. Moreover, for $\forall z_i \in \mathrm{C}$, it holds that

$$\begin{aligned}
&\dot{\delta}_{z_i} e_{z_i}^2 + 2\delta_{z_i} e_{z_i} \dot{e}_{z_i} \\
=&\zeta_{z_i}[\sum_{z_j \in \Omega_{\mathrm{In}}^z} a_{z_i,z_j}(\hat{\lambda}_{z_i} - \hat{\lambda}_{z_j})^2 + \sum_{z_j \in \Omega_{\mathrm{Ex}}^z} a_{z_i,z_j}(\hat{\lambda}_{z_i} - \hat{\lambda}_{z_j})^2] \\
-&2e_{z_i}[\sum_{z_j \in \Omega_{\mathrm{In}}^z} a_{z_i,z_j}(\hat{\lambda}_{z_i} - \hat{\lambda}_{z_j}) + \sum_{z_j \in \Omega_{\mathrm{Ex}}^z} a_{z_i,z_j}(\hat{\lambda}_{z_i} - \hat{\lambda}_{z_j})]
\end{aligned} \tag{A2}$$

where $e_{z_i} = \hat{\lambda}_{z_i}(t) - \lambda_{z_i}(t)$ denotes the error between the actual value and trigger value. $\zeta_{z_i} \in (0,1)$. For convenience, we denote

$$\begin{aligned}
l_{\mathrm{In}}^{z_i} = \sum_{z_j \in \Omega_{\mathrm{In}}^z} a_{z_i,z_j}(\hat{\lambda}_{z_i} - \hat{\lambda}_{z_j})^2, l_{\mathrm{Ex}}^{z_i} = \sum_{z_j \in \Omega_{\mathrm{Ex}}^z} a_{z_i,z_j}(\hat{\lambda}_{z_i} - \hat{\lambda}_{z_j})^2 \\
s_{\mathrm{In}}^{z_i} = \sum_{z_j \in \Omega_{\mathrm{In}}^z} a_{z_i,z_j}(\hat{\lambda}_{z_i} - \hat{\lambda}_{z_j}), s_{\mathrm{Ex}}^{z_i} = \sum_{z_j \in \Omega_{\mathrm{Ex}}^z} a_{z_i,z_j}(\hat{\lambda}_{z_i} - \hat{\lambda}_{z_j}).
\end{aligned} \tag{A3}$$

Therefore, (A2) can be rewritten as

$$\dot{\delta}_{z_i} = \frac{\zeta_{z_i}(l_{\mathrm{In}}^{z_i} + l_{\mathrm{Ex}}^{z_i})}{e_{z_i}^2} - (q\delta_{z_i} c_{z_i} + 1)\frac{2(s_{\mathrm{In}}^{z_i} + s_{\mathrm{Ex}}^{z_i})}{e_{z_i}} \tag{A4}$$

where k is the control parameter, which is a constant.

Let $\boldsymbol{w}_{z_i} = [a_{z_i,z_1}, ..., a_{z_i,z_{n_z}}]^{\mathrm{T}} \in \mathrm{R}^{\mathrm{C}}$ be denoted as the weighted vector of the z_ith node. Denote $\boldsymbol{g}_{z_i} = [\hat{\lambda}_{z_i} - \hat{\lambda}_{z_1}, ..., \hat{\lambda}_{z_i} - \hat{\lambda}_{z_{n_z}}]^{\mathrm{T}} \in \mathrm{R}^{\mathrm{C}}$ as the neighbor error vector. Then,

$$\boldsymbol{w}_{z_i}^{\mathrm{T}} \boldsymbol{g}_{z_i} = s_{\mathrm{In}}^{z_i} + s_{\mathrm{Ex}}^{z_i}, \boldsymbol{g}_{z_i}^{\mathrm{T}} W \boldsymbol{g}_{z_i} = l_{\mathrm{In}}^{z_i} + l_{\mathrm{Ex}}^{z_i} \tag{A5}$$

where $W = \mathrm{diag}(\boldsymbol{w}_{z_i})$. Meanwhile, based on Young's Inequality, combining (A2) and (A5), an inequation can be obtained:

$$\dot{\delta}_{z_i} \geq \underbrace{\frac{\zeta_{z_i} \boldsymbol{g}_{z_i}^{\mathrm{T}} W_{z_i} \boldsymbol{g}_{z_i}}{e_{z_i}^2}}_{J_1} - \underbrace{\frac{\zeta_{z_i} \boldsymbol{g}_{z_i}^{\mathrm{T}} W_{z_i} \boldsymbol{g}_{z_i}}{\kappa_{z_i} e_{z_i}^2}}_{J_2} - \underbrace{\frac{\kappa_{z_i}(1 + q c_{z_i} \delta_{z_i})^2}{\zeta_{z_i}}}_{J_3}$$

To be specific, $\dot{\delta}_{z_i} \geq -J_3$ always holds when $\boldsymbol{g}_{z_i}^{\mathrm{T}} \boldsymbol{W}_{z_i} \boldsymbol{g}_{z_i} = 0$. For another $\boldsymbol{g}_{z_i}^{\mathrm{T}} \boldsymbol{W}_{z_i} \boldsymbol{g}_{z_i} \neq 0$, $\delta_{z_i} \geq -J_3$ is also suitable when $J_1 - J_2 \geq 0$. In this condition, it can be deduced that

$$\kappa_{z_i} \geq \frac{(\boldsymbol{w}_{z_i}^{\mathrm{T}} \boldsymbol{g}_{z_i})^{\mathrm{T}} (\boldsymbol{w}_{z_i}^{\mathrm{T}} \boldsymbol{g}_{z_i})}{\boldsymbol{g}_{z_i}^{\mathrm{T}} W_{z_i}^{\mathrm{T}} \boldsymbol{g}_{z_i}} = \frac{\boldsymbol{g}_{z_i}^{\mathrm{T}} (\boldsymbol{w}_{z_i} \boldsymbol{w}_{z_i}^{\mathrm{T}}) \boldsymbol{g}_{z_i}}{\boldsymbol{g}_{z_i}^{\mathrm{T}} W_{z_i}^{\mathrm{T}} \boldsymbol{g}_{z_i}} \tag{A6}$$

Therefore, $\kappa_{z_i} = \mathrm{eigmax}(\boldsymbol{w}_{z_i}^{\mathrm{T}} \boldsymbol{w}_{z_i}) / \mathrm{eigmin}(W_{z_i})$ is a suitable value, which satisfies

$$d_{\delta_{z_i}} \geq -\frac{\kappa_{z_i}(1 + q c_{z_i} \delta_{z_i})^2}{\zeta_{z_i}} dt \tag{A7}$$

Then, we have

$$\begin{aligned}
\mathcal{T}_{z_i} &= t_{z_i}^{k+1} - t_{z_i}^k \\
&\geq \int_0^{\tilde{\delta}_{z_i}} \frac{\zeta_{z_i}}{\kappa_{z_i}(1 + q c_{z_i} \delta_{z_i})^2} d_{\delta_{z_i}} = \frac{\zeta_{z_i}}{q c_{z_i} \kappa_{z_i}}
\end{aligned} \tag{A8}$$

Based on the above analysis, for $\forall z_i \in \mathrm{C}$, there exists a positive minimal inter-event time

$$\mathcal{T}_{z_i} \geq \frac{\zeta_{z_i} \min_{z_j} a_{z_i,z_j}}{q c_{z_i} \sum_{z_j} a^2_{z_i,z_j}}, \forall z_j \in \Omega^z_{\mathrm{In}} \cup \Omega^z_{\mathrm{Ex}} \tag{A9}$$

Appendix A.2. Proof of Theorem 2

We denote $\Omega_{\mathrm{m}} = \{1, ..., m\}$ as the sequence number set of EB, and the sequence number set of $(m-1)$ energy bodies without the zth EB is denoted as $\Omega^z_{\mathrm{m}} = \{1, ..., z-1, z+1, ...m\}$. Without losing the generality, we take the zth EB as an example. Moreover, the latest trigger vector of $\hat{\lambda}$ and the Laplacian matrix can be redefined as

$$\boldsymbol{\lambda}_{\mathrm{W}} = \begin{bmatrix} \boldsymbol{\lambda}_{\Omega^z_{\mathrm{m}}} \\ \boldsymbol{\lambda}_z \end{bmatrix}, \hat{\boldsymbol{\lambda}}_{\mathrm{W}} = \begin{bmatrix} \hat{\boldsymbol{\lambda}}_{\Omega^z_{\mathrm{m}}} \\ \hat{\boldsymbol{\lambda}}_z \end{bmatrix}, \mathcal{L}_{\mathrm{W}} = \begin{bmatrix} L_{\Omega^z_{\mathrm{m}}} & \tilde{L}_{\bullet,z} \\ \tilde{L}^{\mathrm{T}}_{\bullet,z} & \bar{L}_{z,z} \end{bmatrix} \tag{A10}$$

where $\hat{\boldsymbol{\lambda}}_{\Omega^z_{\mathrm{m}}} = [\hat{\lambda}^{\mathrm{T}}_1, ..., \hat{\lambda}^{\mathrm{T}}_{z-1}, \hat{\lambda}^{\mathrm{T}}_{z+1}, ..., \hat{\lambda}^{\mathrm{T}}_m]^{\mathrm{T}}$, $\boldsymbol{\lambda}_{\Omega^z_{\mathrm{m}}} = [\lambda^{\mathrm{T}}_1, ..., \lambda^{\mathrm{T}}_{z-1}, \lambda^{\mathrm{T}}_{z+1}, ..., \lambda^{\mathrm{T}}_m]^{\mathrm{T}}$, $\hat{\boldsymbol{\lambda}}_z = [\hat{\lambda}_{z_1}, ..., \hat{\lambda}_{z_{n_z}}]^{\mathrm{T}}$, $\boldsymbol{\lambda}_z = [\lambda_{z_1}, ..., \lambda_{z_{n_z}}]^{\mathrm{T}}$. $\mathcal{L}_{\Omega^z_{\mathrm{m}}}$ describes the adjacency relationship of $(|\mathrm{C}| - n_z)$ external nodes in $(m-1)$ energy bodies. $\tilde{L}_{\bullet,z}$ describes the node adjacency relationship between the zth EB and other energy bodies. $\bar{L}_{z,z}$ denotes the node adjacency relationship between n_z internal nodes of the zth EB. Thus, it can be deduced that

$$\dot{\boldsymbol{\lambda}}_{\mathrm{W}}(t) = -F_{\mathrm{W}} \mathcal{L}_{\mathrm{W}} \hat{\boldsymbol{\lambda}}_{\mathrm{W}}(t) \tag{A11}$$

where $\dot{\boldsymbol{\lambda}}_{\mathrm{W}} = [\dot{\boldsymbol{\lambda}}^{\mathrm{T}}_1, ..., \dot{\boldsymbol{\lambda}}^{\mathrm{T}}_{z-1}, \dot{\boldsymbol{\lambda}}^{\mathrm{T}}_{z+1}, ..., \dot{\boldsymbol{\lambda}}^{\mathrm{T}}_m, \dot{\boldsymbol{\lambda}}^{\mathrm{T}}_z]^{\mathrm{T}}$ and $\dot{\boldsymbol{\lambda}}_z = [\dot{\lambda}_{z_1}, ..., \dot{\lambda}_{z_{n_z}}]^{\mathrm{T}}$. The diagonal coefficient matrix can be defined as

$$F = \mathrm{diag}\{2q\mathcal{C}_1, ..., 2q\mathcal{C}_{z-1}, 2q\mathcal{C}_{z+1}, ..., 2q\mathcal{C}_m, 2q\mathcal{C}_z\} \tag{A12}$$

where $\mathcal{C}_z = [c_{z_1}, ..., c_{z_{n_z}}]$.

Meanwhile, to verify the convergence of the proposed distributed strategy, a Lyapunov function is constructed as

$$V(\boldsymbol{\lambda}_{\mathrm{W}}) = \frac{1}{2}(\boldsymbol{\lambda}_{\mathrm{W}} - \widehat{\boldsymbol{\lambda}}_{\mathrm{W}})^{\mathrm{T}} F^{-1}_{\mathrm{W}} (\boldsymbol{\lambda}_{\mathrm{W}} - \widehat{\boldsymbol{\lambda}}_{\mathrm{W}}) \tag{A13}$$

with $\widehat{\lambda} = \frac{1}{|\mathrm{C}|} \mathbb{1}^{\mathrm{T}}_{|\mathrm{C}|} [\boldsymbol{\rho}_{\Omega^z_{\mathrm{M}}} \odot \boldsymbol{\lambda}_{\Omega^z_{\mathrm{M}}}, \boldsymbol{\rho}_z \odot \boldsymbol{\lambda}_z] \mathbb{1}_{|\mathrm{C}|}$, where $\boldsymbol{\rho}_{\Omega^z_{\mathrm{M}}}$ and $\boldsymbol{\rho}_z$ are the coefficient vector of the external nodes in $(m-1)$ energy bodies and the internal nodes of the zth nodes, respectively. $\odot$ is the point multiplication symbol. Moreover, $\boldsymbol{\rho}_{\Omega^z_{\mathrm{M}}} = [\boldsymbol{\rho}^{\mathrm{T}}_1, ..., \boldsymbol{\rho}^{\mathrm{T}}_{z-1}, \boldsymbol{\rho}^{\mathrm{T}}_{z+1}, ..., \boldsymbol{\rho}^{\mathrm{T}}_m]^{\mathrm{T}}$, $\boldsymbol{\rho}_z = [1/(c_{z_1} c^*, ..., 1/(c_{z_{n_z}} c^*)]^{\mathrm{T}}$, where the average parameter c^* can be expressed as

$$c^* = \frac{1}{|\mathrm{C}|} \Big(\sum_{z_i \in \Omega^z_{\mathrm{In}}} c_{z_i} + \sum_{z_i \in \Omega^z_{\mathrm{Ex}}} c_{z_i} \Big) \tag{A14}$$

Meanwhile,

$$\begin{aligned} \dot{V}(\boldsymbol{\lambda}_{\mathrm{W}}) &= \boldsymbol{\lambda}^{\mathrm{T}}_{\mathrm{W}}(t) F^{-1}_{\mathrm{W}} \dot{\boldsymbol{\lambda}}^{\mathrm{T}}_{\mathrm{W}}(t) - \widehat{\boldsymbol{\lambda}}^{\mathrm{T}}_{\mathrm{W}}(t) F^{-1}_{\mathrm{W}} \dot{\boldsymbol{\lambda}}^{\mathrm{T}}_{\mathrm{W}}(t) \\ &= -\boldsymbol{\lambda}^{\mathrm{T}}_{\mathrm{W}}(t) \mathcal{L}_{\mathrm{W}} \hat{\boldsymbol{\lambda}}_{\mathrm{W}}(t) + \widehat{\boldsymbol{\lambda}}^{\mathrm{T}}_{\mathrm{W}}(t) \mathcal{L}_{\mathrm{W}} \hat{\boldsymbol{\lambda}}_{\mathrm{W}}(t) \\ &= -\boldsymbol{\lambda}^{\mathrm{T}}_{\mathrm{W}}(t) \mathcal{L}_{\mathrm{W}} \hat{\boldsymbol{\lambda}}_{\mathrm{W}}(t) \end{aligned} \tag{A15}$$

Recalling that $\boldsymbol{\lambda}(t) = \hat{\boldsymbol{\lambda}}(t) - \boldsymbol{e}(t)$, we have

$$\begin{aligned} \dot{V}(\boldsymbol{\lambda}_{\mathrm{W}}) &= -\hat{\boldsymbol{\lambda}}^{\mathrm{T}}_{\mathrm{W}}(t) \mathcal{L}_{\mathrm{W}} \boldsymbol{\lambda}_{\mathrm{W}}(t) + e^{\mathrm{T}}_{\mathrm{W}}(t) \mathcal{L}_{\mathrm{W}} \hat{\boldsymbol{\lambda}}^{\mathrm{T}}_{\mathrm{W}}(t) \\ &\leq -\frac{1}{2} \sum_{z_i \in \mathrm{C}} [(l^{z_i}_{\mathrm{In}} + l^{z_i}_{\mathrm{Ex}}) - 2e^2_{z_i}(t)] \end{aligned} \tag{A16}$$

Based on the event-triggered mechanism proposed in **Algorithm 1**, it is obvious that

$$\dot{V}(\boldsymbol{\lambda}_{\mathrm{W}}) \leq -\frac{1-\kappa_{max}}{2}\hat{\boldsymbol{\lambda}}_{\mathrm{W}}^{\mathrm{T}}(t)\mathcal{L}_{\mathrm{W}}\hat{\boldsymbol{\lambda}}_{\mathrm{W}}(t) \tag{A17}$$

where $\kappa_{max} = max\{\kappa_{z_i}, \kappa_{z_j} | z_i \in \Omega_{\mathrm{In}}^{z}, z_j \in \Omega_{\mathrm{Ex}}^{z}\}$.

According to the analysis above, the convergence of the proposed distributed seaport energy management strategy is verified.

References

1. Duarte, C.; Agusti, S.; Barbier, E.; Britten, G.; Castilla, J.; Fulweiler, R.; Hughes, T.; Knowlton, N.; Lovelock, H.; Lotze, C.; et al. Rebuilding Marine Life. *Nature* **2020**, *580*, 39–51.
2. Choudhary, P.; Subhash, G.; Khade, M.; Savant, S.; Musale, A.; Kumar, G.; Chelliah, M.; Dasgupta, S. Empowering Blue Economy: From Underrated Ecosystem to Sustainable Industry. *J. Environ. Manag.* **2021**, *291*, 112697.
3. Iris, C.; Lam, J. A review of energy efficiency in ports: Operational strategies, technologies, and energy management systems. *Renew. Sustain. Energ. Rev.* **2019**, *112*, 170–182.
4. Kohl, M.; Linser, S.; Prins, K.; Talarczyk, A. The EU Climate Package "Fit for 55"—A Double-Edged Sword for Europeans and Their Forests And Timber Industry. *For. Policy Econ.* **2022**, *132*, 102596.
5. Ovaere, M.; Proost, S. Cost-Effective Reduction of Fossil Energy Use in The European Transport Sector: An Assessment of The Fit for 55 Package. *Energy Policy* **2022**, *168*, 113085.
6. Wang, R.; Sun, Q.; Ma, D.; Hu, X. Line Impedance Cooperative Stability Region Identification Method for Grid-Tied Inverters Under Weak Grids. *IEEE Trans. Smart Grid* **2020**, *11*, 2856–2866.
7. Wang, C.; Zhang, Z. Energy-efficient time synchronisation based on odd-even periodic data transmission and acknowledgement in wireless sensor networks. *Int. J. Sens. Netw.* **2022**, *38*, 113–121.
8. Wang, L.; Li, M.; Wang, Y.; Chen, Z. Energy Management Strategy and Optimal Sizing for Hybrid Energy Storage Systems Using an Evolutionary Algorithm. *IEEE T. Intell. Transp.* **2022**, *23*, 14283–14293.
9. Zhou, W.; Zhang, N.; Zhai, H. Enhanced Battery Power Constraint Handling in MPC-Based HEV Energy Management: A Two-Phase Dual-Model Approach. *IEEE Trans. Transp. Electr.* **2021**, *7*, 1236–1248.
10. Sun, Q. *Energy Internet and We-Energy*; Springer: Singapore, 2019.
11. Li, Y.; Wang, F.; Tang, X.; Lin, X.; Liu, C.; Hu, X. Real-Time Multi-objective Energy Management for Electrified Powertrains: A Convex Optimization-Driven Predictive Approach. *IEEE Trans. Transp. Electrif.* **2022**, *8*, 3139–3150.
12. Zhang, G.; Hu, W.; Cai, D.; Zhang, Z.; Huang, Q.; Chen, Z.; Blaabjerg, F. A multi-agent deep reinforcement learning approach enabled distributed energy management schedule for the coordinate. *Energy Convers. Manag.* **2022**, *255*, 115340.
13. Huang, B.; Li, Y.; Zhan, F.; Sun, Q.; Zhang, H. A distributed robust economic dispatch strategy for integrated energy system considering cyber-attacks. *IEEE Trans. Ind. Inform.* **2022**, *18*, 880–890.
14. Li, Y.; Li, T.; Zhang, H.; Xie, X.; Sun, Q. Distributed resilient double-gradient-descent based energy management strategy for multi-energy system under DoS attacks. *IEEE Trans. Netw. Sci. Eng.* **2022**, *9*, 2301–2316.
15. International Maritime Organization (IMO). *Procedures for Port State Control*; A.1155; International Maritime Organization (IMO): London, UK, 2021.
16. Fang, S.; Wang, Y.; Gou, B.; Xu, Y. Toward future green maritime transportation: An overview of seaport microgrids and all-electric ships. *IEEE Trans. Veh. Technol.* **2020**, *69*, 207–219.
17. Alvarez, P. From maritime salvage to IMO 2020 strategy: Two actions to protect the environment. *Mar. Pollut. Bull.* **2021**, *170*, 112590.
18. Wu, P.; Lin, C. Cost-Benefit Evaluation on Promising Strategies in Compliance with Low Sulfur Policy of IMO. *J. Mar. Sci. Eng.* **2021**, *9*, 3.
19. Sun, X.; Qiu, J. Hierarchically Coordinated Voltage Control in Seaport Microgrids Considering Optimal Voyage Navigation of All-Electric Ships. *IEEE Trans. Transp. Electrif.* **2022**, *8*, 2191–2204.
20. Garcia, B.; Foerster, A.; Lin, J. Net Zero for the International Shipping Sector? An Analysis of the Implementation and Regulatory Challenges of the IMO Strategy on Reduction of GHG Emissions. *J. Environ. Law* **2021**, *33*, 85–112.
21. Song, J.; Shan, Q.; Zou, T.; Hu, J.; Teng, T. Distributed Energy Management for Zero-Carbon Port Microgrid. *Int. Trans. Electr. Energy Syst.* **2022**, *2022*, 2752802.
22. Shivam, K.; Tzou, J.; Wu, S. A multi-objective predictive energy management strategy for residential grid-connected PV-battery hybrid systems based on machine learning technique. *Energy Convers. Manag.* **2021**, *237*, 114103.
23. Merabet, A.; Al-Durra, A.; El-Saadany, E. Energy management system for optimal cost and storage utilization of renewable hybrid energy microgrid. *Int. Trans. Electr. Energy* **2022**, *252*, 115116.
24. Wang, J.; Xiao, Y.; Li, T.; Chen, C.L.P. A Survey of Technologies for Unmanned Merchant Ships. *IEEE Access* **2020**, *8*, 224461–224486. https://doi.org/10.1109/ACCESS.2020.3044040
25. Wang, J.; Xiao, Y.; Li, T.; Philip Chen, C.L. Impacts of GPS Spoofing on Path Planning of Unmanned Surface Ships. *Electronics* **2022**, *11*, 801. https://doi.org/10.3390/electronics11050801

26. Maleki, Z.; Maleki, H.; Akbari, R. A bi-level mathematical model to protect gateways in underwater wireless sensor networks. *Int. J. Sens. Netw.* **2022**, *40*, 85–93.
27. Xu, Y.; Li, T.; Yang, Y.; Shan, Q.; Tong, S.; Philip Chen, C.L. Anti-attack event-triggered control for nonlinear multi-agent systems with input quantization. *IEEE Trans. Neural Netw. Learn. Syst.* **2022**, Early Access.
28. Li, Y.; Gao, D.W.; Gao, W.; Zhang, H.; Zhou, J. Double-mode energy management for multi-energy system via distributed dynamic event-triggered newton-raphson algorithm. *IEEE Trans. Smart Grid* **202**, *11*, 5339–5356.
29. Li, Y.; Zhang, H.; Liang, X.; Huang, B. Event-Triggered-Based Distributed Cooperative Energy Management for Multienergy Systems. *IEEE Trans. Ind. Inform.* **2019**, *15*, 2008–2022.
30. Krivokapic, R. Perspectives for the Development of Small Seaports with Reference to the Adriatic Seaports. *Transform. Bus. Econ.* **2022**, *21*, 21–33.
31. Teng, F.; Zhang, Q.; Zou, T.; Zhu, J.; Tu, Y.; Feng, Q. Energy Management Strategy for Seaport Integrated Energy System under Polymorphic Network. *Sustainability* **2023**, *15*, 53.
32. Peng, X.; Luo, L.; Liao, H.; Zavadskas, E.K.; Al-Barakati, A. A novel Decision-making Method for Resilient Supplier Selection during COVID-19 Pandemic Outbreak based on Hesitant Fuzzy Linguistic Preference Relations. *Transform. Bus. Econ.* **2021**, *20*, 238–258.
33. Iris, C., Lam, J.S.L. Optimal energy management and operations planning in seaports with smart grid while harnessing renewable energy under uncertainty. *OMEGA Int. J. Manag. Sci.* **2021**, *103*, 102445.
34. Yigit, K.; Acarkan, B. A New Electrical Energy Management Approach for Ships Using Mixed Energy Sources to Ensure Sustainable Port Cities. *Sustain. Cities Soc.* **2018**, *40*, 126–135.
35. Roy, A.; Auger, F.; Olivier, J.C.; Schaeffer, E. Auvity B. Design, Sizing, and Energy Management of Microgrids in Harbor Areas: A Review. *Energies* **2020**, *13*, 5314.
36. Jones, A.; Alleway, H.; McAfee, D.; Reis-Santos, P.; Theuerkauf, S.; Jones, R. Climate-Friendly Seafood: The Potential for Emissions Reduction and Carbon Capture in Marine Aquaculture. *Bioscience* **2022**, *72*, 123–143.
37. Sun, Q.; Han, R.; Zhang, H.; Zhou, J.; Guerrero, J. A Multiagent-Based Consensus Algorithm for Distributed Coordinated Control of Distributed Generators in the Energy Internet. *IEEE Trans. Smart Grid* **2015**, *6*, 3006–3019.
38. Wang, F.; Teng, F.; Xiao, G.; He, Y.; Feng, Q. Resilient Distributed Secondary Control Strategy for Polymorphic Seaport Microgrid against Estimation-Dependent FDI Attacks. *J. Mar. Sci. Eng.* **2022**, *10*, 1668.